Environmental Toxicology and Chemistry—Volume 38, Number 8—pp. 1738–1747, 2019
Received: 19 February 2019 | Revised: 20 March 2019 | Accepted: 14 May 2019

Environmental Toxicology

Performance of Three-Dimensional Rainbow Trout (*Oncorhynchus mykiss*) Hepatocyte Spheroids for Evaluating Biotransformation of Pyrene

Maria Therese Hultman,* Katharina Bjarnar Løken, Merete Grung, Malcolm J. Reid, and Adam Lillicrap

Norwegian Institute for Water Research, Oslo, Norway

Abstract: The aquatic bioconcentration of a chemical is typically determined using conventional fish tests. To foster the approach of alternatives to animal testing, a combination of computational models and in vitro substrate depletion bioassays (e.g., primary hepatocytes) can be used. One recently developed in vitro assay is the three-dimensional (3D) hepatic spheroid model from rainbow trout (*Oncorhynchus mykiss*). The aim of the present study was to evaluate the metabolic competence of the 3D spheroids from rainbow trout when exposed to pyrene, using 2 different sampling procedures (SP1 and SP2). The results were compared with previously published intrinsic clearance (CL) results from S9 fractions and primary hepatocyte assays. Extraction of pyrene using SP1 suggested that the spheroids had depleted 33% of the pyrene within 4 h of exposure, reducing to 91% after 30 h. However, when applying SP2 a substantial amount (36%) of the pyrene was bound to the exposure vial within 2 h, decreasing after 6 h of exposure. Formation of hydroxypyrene-glucuronide (OH-PYR-Glu) was obtained throughout the study, displaying the metabolic competence of the 3D spheroids. The 2 sampling procedures yielded different $CL_{in\ vitro}$, where pyrene depletion using SP2 was very similar to published studies using primary hepatocytes. The 3D spheroids demonstrated reproducibile, log-linear biotransformation of pyrene and displayed formation of OH-PYR-Glu, indicating their metabolic competence for 30 h or more. *Environ Toxicol Chem* 2019;38:1738–1747. © 2019 The Authors. *Environmental Toxicology and Chemistry* published by Wiley Periodicals, Inc. on behalf of SETAC.

Keywords: In vitro; Three-dimensional spheroids; Biotransformation; Pyrene; Bioconcentration

INTRODUCTION

Organic compounds in the aquatic environment are of concern if they fulfill one or more of the criteria for being a persistent, bioaccumulative, or toxic substance. Bioaccumulation of hydrophobic organic compounds may occur in aquatic organisms such as fish. The assessment of a compound's potential to bioconcentrate is currently based on its physicochemical properties (e.g., $\log_{KOW}$ as a surrogate metric for the propensity of a chemical to partition into the fats of fish) and subsequently its biotransformation potential, using conventional animal test methods such as fish (e.g., Organisation for Economic Co-operation and Development [OECD] Test Guideline 305). In vivo testing gives rise to both ethical and economic concerns because full bioconcentration studies use large numbers of experimental animals (e.g., 81 fish/study; Lillicrap et al. 2016b) and require dedicated testing facilities. Alternatives to these test methods have been requested (Schirmer 2006; Rovida and Hartung 2009; Scholz et al. 2013; Lillicrap et al. 2016a). To accommodate these requests, computational (in silico) nonanimal models such as quantitative structure–activity relationships have been used to assess a compound's potential to bioconcentrate in aquatic vertebrates (fish; Scholz et al. 2013). Unfortunately, there are large knowledge gaps in some of these computational predictive models because many chemical domains are not fully covered by experimental information or are not able to account for biotransformation (Arnot and Gobas 2006; Johanning et al. 2012). However, recent developments of computational models have successfully predicted biotransformation rate constants for several compounds in fish (Arnot et al. 2009; Papa et al. 2014), although further refinement is still warranted.

In an effort to further improve the predictions of currently existing computational models and endorse the refinement, reduction, and replacement (3Rs) of animal testing, a battery of well-established in vitro tests (e.g., S9 fractions, primary hepatocyte

This article contains online-only Supplemental Data.

* Address correspondence to mhu@niva.no
Published online 17 May 2019 in Wiley Online Library (wileyonlinelibrary.com).
DOI: 10.1002/etc.4476

cells, and continuous cell lines) have been evaluated for their applicability as alternatives to complement conventional in vivo bioaccumulation models (Fay et al. 2014a, 2014b; Embry et al. 2015; Fay et al. 2017; Stadnicka-Michalak et al. 2018). Recently, OECD guidance documents concerning the use of in vitro assays for extrapolation to in vivo intrinsic clearance were published (OECD 2018). These OECD test guidelines (319A and 319B) describe the use of S9 fractions and cryopreserved hepatocytes from rainbow trout (*Oncorhynchus mykiss*). The test guidelines were the result of an international ring trial (Nichols et al. 2018) that tested a broad range of hydrophobic compounds including the model compound pyrene. This polycyclic aromatic hydrocarbon (PAH) is a nonpolar and nonionic compound with intermediate hydrophobicity ($\log_{KOW}$ 4.88) and is therefore a suitable model compound to use in intrinsic clearance (CL) assays.

Identification of highly metabolically active hepatic in vitro models accommodating biotransformation of PAHs (e.g., pyrene) as described in fish livers through phase I (mostly oxidation) reactions forming 1-hydroxypyrene (OH-PYR) and its further conjugation through phase II biotransformation (e.g., UDP-glucuronosyltransferase or sulfotransferase; Van der Oost et al. 2003) into 1-hydroxypyrene-glucuronide (OH-PYR-Glu) and/or pyrene-sulfate (Ikenaka et al. 2013) is highly warranted. Such in vitro model is the three-dimensional (3D) hepatic spheroid culture that is well established in mammalian pharmacology and cancer research because it has been suggested to better reflect in vivo exposure and organ response than monolayer cell cultures (Elliott and Yuan 2011; Kyffin et al. 2018). The spheroid model has shown promise in prolonged duration of exposure (>72 h; Hoffmann et al. 2015; Baron et al. 2017; Ramaiahgari et al. 2017), enabling tests of slowly metabolizing compounds that previously had been a challenge for well-established in vitro bioassays (e.g., S9 and primary hepatocytes) because of their shorter shelf life (i.e., reduced viability over extended durations). In addition, the spheroid model may better reflect in vivo tissue activity and functionality because its microenvironment, cellular ultrastructure, metabolic competence, and toxicity response is improved compared with 2D-based assays (Kyffin et al. 2019; Lammel et al. 2019). The 3D hepatic spheroid model was not established in fish until recently, using primary cells from rainbow trout that have successfully been used in biotransformation studies of selected pharmaceuticals (Baron et al. 2012; Baron et al. 2017). The 3D model has since been developed for different cells of origin (primary cells and continuous cell lines) in fish and has been used in investigation of toxic effects and metabolism of xenobiotic compounds and pharmaceuticals (Uchea et al. 2015; Langan et al. 2018; Lammel et al. 2019). However there are very few studies, apart from those involving pharmaceuticals, that have evaluated the ability of 3D hepatic spheroids to metabolize environmentally relevant organic compounds (Uchea et al. 2015).

The aim of the present study was to evaluate the biotransformation performance of 3D hepatic spheroid cultures from rainbow trout, and to compare the results with other experimental in vitro models assessing biotransformation (such as S9 fractions and primary hepatocytes from rainbow trout). Pyrene was used as the test substance to characterize the spheroid culture's metabolic performance, and to determine its possible applicability as an alternative in vitro model to assess compounds' biotransformation. To test the in vitro model's metabolic capacity, both parent pyrene and its transformation products were measured at the end of the exposure period. The measured transformation products were OH-PYR and OH-PYR-Glu. Moreover, the concentration of pyrene was assessed throughout the exposure period in spheroid/media and the test vessel because the intermediate $\log_{KOW}$ may affect the total amount of chemical in solution during the duration of exposure. The spheroid's biotransformation capacity was thereafter compared with other in vitro biotransformation models such as the S9 fractions and primary hepatocytes from rainbow trout as reported in Organisation for Economic Co-operation and Development (2018).

MATERIALS AND METHODS

Test chemicals

The test chemical pyrene (purity 98%; CAS 129-00-0) was purchased from Sigma-Aldrich. Acetone (purity ≥ 99.9%; CAS 67-64-1) and acetonitrile (purity ≥ 99.95%; CAS 75-05-8) were obtained from VWR. β-glucuronidase/aryl sulfatase was purchased from Merck. A concentrated stock solution of pyrene (5 mM) used for the biotransformation assays was dissolved in acetone and stored for a maximum of 2 wk in the dark at −20 °C before use.

Fish

Sexually immature rainbow trout (200–500 g) were obtained from Valdres Ørretoppdrett and reared at the Department of Biosciences at the University of Oslo for a minimum of 4 wk before the start of the study. The fish were maintained in tap water at 8 ± 2 °C, pH 6.6 at a regime of 12:12-h, light:dark cycle. Fish were fed daily with commercial pellets (Skretting) ad libitum.

3D spheroid cultivation

A total of 6 fish were collected (from September–November 2016) and humanely terminated with a blow to the head, followed by immediate dissection to expose the abdominal cavity and the lateral abdominal vein. Only immature fish with no visually matured gonads were subjected to a 2-step hepatic cell isolation procedure by perfusion through the lateral abdominal vein/hepatic portal vein, as previously described by Tollefsen et al. (2003). Viability (>90%) of the isolated primary hepatocytes was assessed using a Bürker-Türk counting chamber and Trypan blue:cell suspension (2:1, v/v). The hepatocyte suspension was diluted to 1×10^6 cells/mL in Leibovits 15 (L-15) media (with L-glutamine, without phenol) supplemented with sterile 10% foetal bovine serum, amphotericin (0.25 g/mL), streptomycin (100 mg/mL), penicillin (100 U/mL), and $NaHCO_3$ (4.5 mM). The cell suspension was seeded by dispensing 3 mL into separate wells of a 6-well plate pre-coated with 2.5% pHEMA to avoid any surface attachment, as earlier described by Baron et al. (2012). The cell plates were thereafter placed on an orbital shaker (Mini Shaker-15; VWR) at 78 rpm and incubated in an ambient atmosphere at 15 °C until the spheroids

reached maturity (>8 d; Baron et al. 2012). Culture media was changed within 24 h of cell isolation and thereafter 3 times per wk. Preparation of pHEMA pre-coated cell plates and all cell-related activities after cell isolation were carried out in a HEPA filter (Class II) laminar flow sterile cabinet (Holten LaminAir Model 1.5). The spheroids were evaluated by visual inspection under a light microscope to ensure maturity was reached within 7 to 8 d, and were viable up to 37 d after seeding (Figure 1).

Preparation of spheroids for exposure

Once maturity was reached, 10- to 18-d old spheroids with a diameter between 90 to 150 µm were carefully collected using a cut-off pipette tip and dispensed into a sterile Falcon tube that was centrifuged at 300 rpm for 3 min. The cell media was removed using a pipette and replaced with 15-mL L-15 media without any media supplements. Because the spheroids were too large for a haemocytometer, they were morphologically assessed and counted under a light microscope (×20) in 4 × 10-µL droplets. Once the spheroid concentrations were established, preparations of 50 and 100 spheroids in 140 µL of media (357 and 714 spheroids per mL) were conducted. Aliquots of the different densities of spheroid solutions were also heat-inactivated for 20 min at 100 °C and used as a parallel negative enzymatic control for all the sample time points. Morphological integrity and cell viability were continuously assessed (at 0, 2, 4, 6, 24, and 30 h) during the experiment.

Chemical exposure

The 5-mM pyrene concentrated stock solution was diluted to a 50-µM pyrene stock solution using acetone on the experimental start day, and further diluted to 50 nM (0.1% acetone) in an intermediate stock that was added to the 3D spheroid solution, reaching a final concentration of 25 nM (0.05% acetone) in L-15 media without any additional supplements. An independent experiment was performed to chemically verify any loss of the total amount of pyrene in the intermediate stock solution (50 nM pyrene) during the dilution step after 1 h of incubation, using acetone, reverse osmosis water (RO-H_2O), and L-15 media as dilution buffers. To further investigate whether pyrene was binding to the test vessel (glass vial) over the duration of exposure, an additional test was performed where 250 nM pyrene were spiked into an L-15 solution containing 0.1

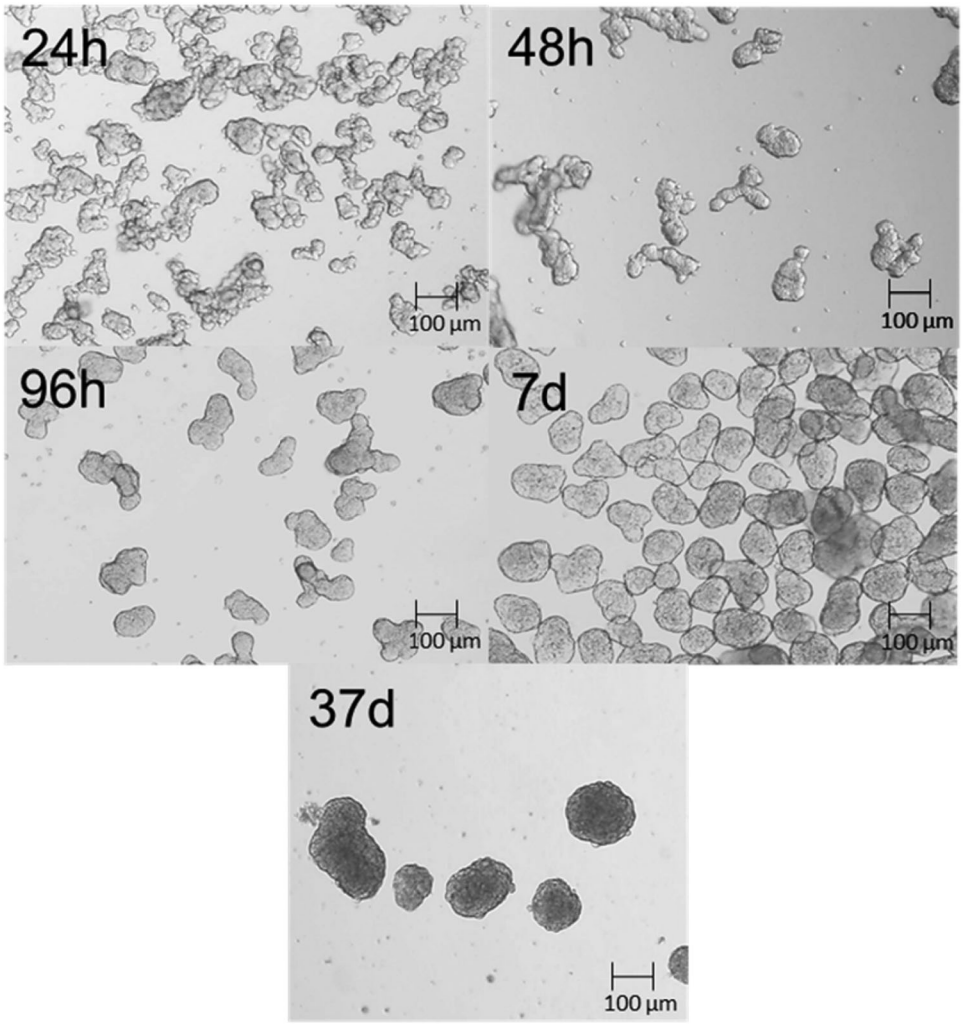

FIGURE 1: Light microscope images taken during aggregation of the rainbow trout (*Oncorhynchus mykiss*) hepatocytes and formation of spheroids from 24 h up to 37 d.

and 1% of bovine serum albumin (BSA) for a period of 0 to 6 h because any chemical loss to the glass should occur within that time.

Independent of previous experiments, the number of spheroids (50 or 100) and duration (0, 0.5, 1, 2, 4, 6, 24, and 30 h) of exposure were evaluated by first dispensing a 140-µL aliquot of live and heat-inactivated spheroids into 4 × 1.5-mL glass vials, respectively, creating 4 technical replicates per exposure time. On exposure, 140 µL of 50 nM pyrene solution were added to the exposure vials, resulting in a final concentration of 25 nM pyrene (0.05% acetone). The spheroids were exposed to 25 nM pyrene for the duration of the exposure. The substrate depletion assay was stopped at the individual time points by extracting one individual replicate by adding 1200-µL, ice-cold acetonitrile in a 1:5 ration of sample:acetonitrile (Organisation for Economic Co-operation and Development 2018).

To obtain optimal log-linear depletion kinetics for the test compound, an assessment of the best sampling strategy was performed to measure compound biotransformation in the vial containing 3D spheroids. The sampling procedure (SP1) was carried out directly in the exposure vials as previously described by Baron et al. (2017) and by moving the spheroids and exposure media into a new vial (SP2). Sampling procedure 1 was conducted to replicate 3D spheroid experiments performed by Baron et al. (2017). Nevertheless, earlier studies (Qian et al. 2011) and chemical analysis indicated that there was likely to be a reduction in the amount of pyrene present in the solution. Accordingly, SP2 was used to determine the total amount of pyrene in the cell media (including spheroids) solution versus the identified amount of pyrene adsorbed to the glass wall of the exposure vial. In short, on stopping the metabolic reaction at each sampling point, all media and spheroids were collected and dispensed into a new vial followed by addition of 1200 µL acetonitrile. Correspondingly, the exposure vial was extracted by adding 1480 µL of acetonitrile to obtain any analyte adhered to the glass vial.

Protein analysis

Protein was analyzed in samples containing BSA using the modified Lowry method (Lowry et al. 1951). In summary, 10 µL of sample and bovine ɤ-globulin protein standard (0.125–1.125 mg/mL diluted in 0.1 M Tris buffer; pH 8.0) were pipetted into a 96-well plate followed by addition of 25 µL of alkaline copper tartrate solution (Bio-Rad) and 200 µL of Folin's reagent (Bio-Rad). The plate was gently mixed and then incubated for 15 min in the dark at room temperature (20 °C). The plate was read at 750-nm absorbance on a VersaMax 96-well microplate reader (Molecular Devices).

Chemical analysis

Chemical analyses of pyrene and its transformation products were performed using a Waters 2695 high-performance liquid chromatography (HPLC) Separations Module attached to a 2475 fluorescence detector. A Waters PAH C18 column (4.6 × 250 mm) with 5-µm particles was used. The mobile phase consisted of a gradient from 40:60 acetonitrile:ammonium acetate (0.05 M; pH 4.1) to 100% acetonitrile at a flow of 1 mL/min. The column was heated to 35 °C. Fluorescence was measured at the following excitation/emission wavelengths: 1-hydroxypyrene β-D-glucuronide 342/380 nm; OH-PYR, and pyrene 346/384 nm. Aliquots of 25-µL samples were injected directly into the HPLC for each analysis. The results were calculated using the external standard method. The calibration standards were obtained from Chiron and were in the range of 0.1 to 10 ng/mL. The procedure was described in detail in Kammann et al. (2013) and showed good results (z score <1) for quantification of OH-PYR in an interlaboratory ring trial. Deconjugation using β-glucuronidase/aryl sulfatase enzyme was performed in several samples to show that OH-PYR was formed during the exposure duration, as previously described in Kammann et al. (2013). β-glucuronidase/aryl sulfatase enzyme was added in a 1:10 ratio (enzyme:sample), mixed thoroughly, and incubated at 37 °C for 1 h before injection. The analytical approach used herein was developed for pyrene and not specifically for the analysis of metabolites OH-PYR and OH-PYR-Glu. Analytical uncertainty associated with the low levels of metabolites observed therefore prevented an appropriate accurate mass-balance calculation.

Determination of in vitro and in vivo hepatic intrinsic CL

The intrinsic CL rate of the spheroids ($CL_{in\ vitro,\ spheroid}$; mL/h/$10^6$ cells) was determined for pyrene using a substrate depletion approach. Measured substrate concentrations of pyrene were log_{10}-transformed and plotted against time (h) to obtain a first-order elimination rate constant ($k = -2.3 \times$ slope; Remington 2006). The $CL_{in\ vitro,\ spheroid}$ was determined by dividing the elimination rate constant by total cell number, approximated as 500 cells/spheroid and thus 5.0×10^4 cells in 100 spheroids per well (Baron et al. 2012). To estimate the in vivo intrinsic CL rate ($CL_{in\ vivo,\ spheroid}$; mL/h/g liver) the $CL_{in\ vitro,\ spheroid}$ value was multiplied by the hepatocellularity value identified as 5.1×10^8 hepatocytes/g liver for sexually immature rainbow trout (Fay et al. 2014a).

Statistical analysis

Statistical analysis was performed on the initial experiment measuring pyrene concentration in the intermediate stock solutions to identify any significant ($p < 0.05$) difference in dissolved pyrene concentration in acetone, L-15, and RO-H_2O. The analysis was performed using GraphPad Prism Ver 5.04 (GraphPad Software) applying analysis of variance with Tukey's post hoc test after the criteria for homogeneity were met.

RESULTS

Chemical analysis

The chemical analysis quantified pyrene (retention time [Rt] 23.1 min), OH-PYR-Glu (Rt 4.2 min), and an unknown pyrene metabolite (Rt 4.8 min) in the exposure media. The unidentified pyrene metabolite appeared as a defined peak in the

chromatogram in some samples, and the levels increased with the duration of exposure. Surprisingly, there was no measurable detection of OH-PYR (Rt 14.1 min) in any of the analyzed samples. However, when performing a deconjugation of the metabolites by β-glucuronidase/aryl sulfatase, a time-dependent (1–30 h) increase of the OH-PYR was detected, displaying measurable levels during the whole duration of exposure (data not shown).

To fully assess the study design and identify any potential loss of compound, analytical chemistry was performed in all dilution steps before exposure. Three different media (acetone, L-15, and RO-H_2O) were tested, assessing the total amount of pyrene present in the solution and adsorbed (not bioavailable) to the glass bottle after 1 h of incubation. There was a slight loss of dissolved compound (50 nM) during the intermediate dilution step, identifying a significant difference ($p < 0.05$) in total amount of pyrene in solution between acetone and RO-H_2O. Despite this difference, both solutions were within the nominal concentration of 50 nM and the amount of dissolved pyrene was therefore not considered to be affected by the media into which it was spiked when used within 1 h of preparation.

The presence of 0.1 and 1% of BSA in the pyrene solution marginally increased the total amount of dissolved pyrene concentration in the media (0–2 h), with 1% BSA having the highest retention capacity after 2 h of incubation (Supplemental Data, Figure S1).

Evaluation of the number of spheroids and exposure duration

The different number of spheroids and exposure periods were both assessed with the aim of ensuring log-linear depletion kinetics for pyrene. It was established that 100 spheroids per reaction primarily had higher replicate reproducibility and were therefore used throughout the study. In addition, the elimination rate (k = –0.050) was higher compared with 50 spheroids (k = –0.010) during 0 to 6 h of exposure to pyrene (Supplemental Data, Figure S2). It was thus decided that 100 spheroids per reaction were sufficient to yield reproducible depletion kinetics of pyrene (coefficient of variation 1.7–13%) in addition to displaying its biotransformation efficiency by formation of OH-PYR-Glu (Supplemental Data, Figure S2). All studies thereafter were performed under conditions that resulted in log-linear depletion kinetics of pyrene.

In the preliminary experiments, the exposure time of 6 h was determined to not be of sufficient duration because 50% or higher depletion of the original pyrene concentration ($t_{half\text{-}life}$ > 6 h) was thought to yield more reproducible results when conducting multiple cell batch experiments (Supplemental Data, Figure S2). The duration of exposure was therefore prolonged to 30 h, resulting in both representative depletion ($t_{30\ h}$ 91%) and a reproducible log-linear metabolic rate of pyrene (Figure 2). There was formation of OH-PYR-Glu during the full duration of pyrene exposure (0–30 h), indicating continuous biotransformation of pyrene (Supplemental Data, Figure S3). Heat-inactivated spheroids were used as a negative control for biotransformation and did not display any biotransformation of pyrene during the full duration of exposure (Figure 2). Cell viability was assessed between 0 through 30 h of exposure duration and ranged from 49 to 78% compared with a parallel untreated control at the end of the experiment (30 h) represented by one technical replicate. This decrease in cell viability suggested that the pyrene concentration may have had a cytotoxic effect on the spheroids; nevertheless, in the present study the spheroids appeared to have retained their metabolic competence throughout the 30 h of exposure because 93 to 96% of the initially spiked-in pyrene was metabolized at the end of the exposure period.

Evaluation of sampling procedure to obtain intrinsic CL

Because the chemical analysis revealed a reduction of dissolved pyrene in the media and spheroid solution not related to the spheroids' biotransformation in SP1, both SP1 and SP2 were applied. Sampling procedure 1 was carried out according to Baron et al. (2017) with some modification, stopping the metabolic activity of the spheroids directly in the exposure vial. This approach involved spiking cold acetonitrile directly into the exposure vessel and provided a measure of the total amount of analyte(s) in the system either bound within the spheroids or to media constituents, freely dissolved in the media, or bound to the glass exposure vessel. In sampling procedure 2, the media and spheroids were transferred from the exposure vessel and spiked directly into a volume of cold acetonitrile. This process was done to make the design of the 3D spheroid study more comparable with earlier compound depletion studies utilizing primary hepatocytes and S9 fractions (Fay et al. 2014b; Fay et al. 2017; Nichols et al. 2018). Sampling procedure 2 provided only a measure of the amount of analyte within the spheroid bound to media constituents and dissolved in the media. Hence it did not cover the proportion of the analyte(s) that might have been bound to the surface of the exposure vessel.

Figure 2 details the results of SP1, whereas Figure 3 shows the kinetics of SP2. Sampling procedure 1 disclosed first-order

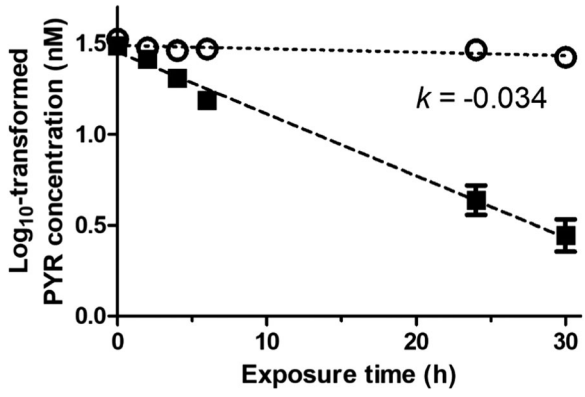

FIGURE 2: Assessment of optimal exposure time to determine substrate depletion kinetics of 25 nM pyrene (PYR). The graph displays the clearance of pyrene (■) in alive and heat-inactivated (○) 3D spheroids. The data represent the mean (±standard error) of 3–4 technical replicates consisting of 100 spheroids each collected from one fish. k = rate constant.

kinetics throughout the duration of the exposure (0–30 h). The spheroids depleted 33% of the original spiked pyrene within 4 h of exposure, further metabolizing a total of 50, 85, and 91% after 6, 24, and 30 h, respectively (Figure 2). Sampling procedure 2, on the other hand, showed an apparent change in the kinetics over time, clearly not being at equilibrium until after 6 h of exposure to pyrene (Figure 3). There was a steep depletion of the total amount of pyrene in the media + spheroid between 0 to 4 h followed by an increase again after 6 h of exposure, representing a depletion of 82 and 84% within the first 2 and 4 h of exposure, respectively (Figure 3). However, in analyzing the pyrene adhered to the glass vial, 36% of the originally added pyrene was adsorbed to the glass wall within 2 h of exposure. Correcting for the pyrene adhered to the glass, the calculated depletion of pyrene by the 3D spheroids was 46 and 58% of the originally spiked-in compound after 2 and 4 h, respectively. The total amount of pyrene in the spheroid + media compartment was, after 6 h of exposure, depleted in a log-linear manner until the end of the exposure (30 h). The pyrene continued to be adsorbed to the glass at quantities of 33 and 2% for the duration of 6 and 24 h, respectively (Supplemental Data, Figure S4). However, based on the depletion rate of pyrene adhered to the glass, this was not a rate-limiting factor for metabolism of pyrene by the spheroids.

Similarly, OH-PYR-Glu also had a high affinity for the glass wall of the vessel during the full duration of the test (Supplemental Data, Figure S4). Heat-inactivated spheroids displayed a decrease in pyrene concentration over time when combining the 2 compartments (spheroids + media and vial (Figure 3)). Nonetheless, this reduction of pyrene was inconsistent over time and because it previously showed not to be an artefact (Figure 2), it was regarded as a confounding factor associated with the chemical analysis and/or recovery of all compound in the different compartments during SP2.

Overall, the intercell batch variation of biotransformation efficiency (regardless of sampling procedure) varied between 16 to 48% coefficient of variation during the 30-h exposure, and was the least variable at 2 h of exposure (16%). The 2 different sampling procedures did however yield similar elimination rates for pyrene when analyzing the whole exposure vial (k = –0.034) versus the spheroid + media (k = –0.042). However, to be comparable with previous in vitro work on pyrene depletion, the elimination rate of total amount of pyrene in measured spheroid + media was used to calculate the intrinsic CL of pyrene in 3D spheroids.

Calculation of intrinsic CL of spheroids ($CL_{in\ vitro,\ spheroid}$) and extrapolation to in vivo ($CL_{in\ vivo,\ spheroid}$)

The in vitro intrinsic CL rate of pyrene by 3D spheroids was very similar to previously published studies using cryopreserved hepatocytes (Table 1). Similarities between the 3D spheroids and cryopreserved hepatocytes were also evident when extrapolating the results to estimates of in vivo intrinsic CL. Comparisons between 3D spheroids and S9 fractions, however, showed larger differences in estimated in vivo intrinsic CL (Table 1).

DISCUSSION

The primary objective of the present study was to evaluate the performance and reproducibility of an in vitro substrate depletion assay using a 3D rainbow trout hepatic spheroid model. To the knowledge of the authors, there have been no previous studies that investigated the 3D spheroid model's biotransformation capacity of pyrene and the formation of the presumed metabolites OH-PYR and OH-PYR-Glu.

Experimental data to evaluate the suitable number of spheroids and the duration of exposure suggested that 100 spheroids per reaction and an exposure duration of 30 h yielded the most reproducible data. This was consistent with a previously published study by Baron et al. (2017). However, during the investigation of the suitable number of spheroids there were differences between the clearance rate constant (k) obtained from 50 and 100 spheroids (Supplemental Data, Figure S2). As a result of a lack of information in the literature, it is not possible to determine why this is occurring. The authors suggest there could be at least 2 explanations: 1) there was not an excess of biotransformation enzyme in the spheroid system, a hypothesis that might be verified if a plateau was observed in k after experiments with increasing numbers of spheroids (e.g., 150, 200, 250, etc.), and/or 2) there was an excess of biotransformation enzyme even at the reaction using 50 spheroids but the rate was limited by another factor such as available surface area or other factors associated with the spheroid microenvironment. Langan et al. (2018) recently proposed that spheroid size is a possible contributing factor to lower metabolism of the test compound because of an effect on the internal oxygen diffusion into the inner layer of larger (>400 μm) as compared with smaller (<200 μm) spheroids. To ensure that the spheroids' viability and basic cellular activity were not limited by their microenvironment (e.g., anoxia in the center of the spheroid), spheroid sizes of 90 to 150 μm in diameter were used in all experiments conducted. This suggests that oxygen consumption was probably not the determining factor affecting the metabolism/clearance rate of

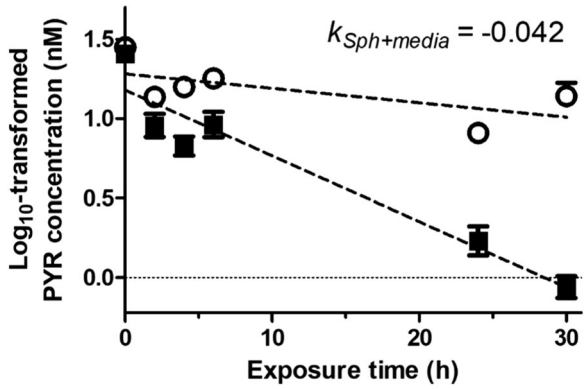

FIGURE 3: Evaluation of biotransformation of 25 nM pyrene (PYR) during 30 h of exposure when separating spheroids (sph) + media from the exposure vial before stopping the reaction. The graph denotes the clearance of pyrene when separately stopping the reaction in spheroids + media (■). Heat-inactivated 3D spheroids (○) are calculated for the whole vial. The data represents the mean (±standard error) of 2 independent assays, each consisting of 100 spheroids per 3-4 technical replicate. k = rate constant.

TABLE 1: Intrinsic hepatic clearance of pyrene by 3D spheroids[a] in comparison with published data on freshly isolated hepatocytes, cryopreserved hepatocytes, and S9 fractions from rainbow trout (*Oncorhynchus mykiss*)

		Measured values for in vitro intrinsic clearance					Extrapolation to in vivo intrinsic clearance			
			Hepatocytes (mL/h/10^6 cells)				Hepatocytes (mL/h/g liver)			
	log_{KOW}	Substrate concn. (nM)	Spheroid sph + media[b]	Fresh[c]	Cryopreserved[d]	S9 (mL/h/mg protein)	Spheroid sph + media[b]	Fresh[c]	Cryopreserved[d]	S9 (mL/h/g liver)
Pyrene	4.88	25	1.9	NR	1.9 ± 0.4[f];3.5[i]	19.5 ± 4.4;20.98[i]	985		964 ± 433[f]	2603 ± 443[f]
		250	NR	3.9 ± 0.9[g]	3.1 ± 1.0[e]	NR	NR	1989[h]	1580 ± 500[e]	

[a]Exposure duration of 0–30 h.
[b]In vitro intrinsic clearance measured in hepatocyte spheroids by stopping the reaction in a separate new vial.
[c]In vitro intrinsic clearance calculated using freshly isolated hepatocytes.
[d]In vitro intrinsic clearance measured using cryopreserved hepatocytes.
[e]CLogP estimated values from: Fay et al. 2017.
[f]Organisation for Economic Co-operation and Development 2018.
[g]Fay et al. 2014a.
[h]Estimated value based on $CL_{in\ vitro,\ int.\ Fresh\ Hep.}$ result from: Fay et al. 2014a.
[i]Nichols et al. 2018.
CL = intrinsic clearance; NR = not recorded.

pyrene in the present study. Apart from a potential impact by the oxygen-regulated microenvironment, the size-dependent metabolic rate might also be caused by the lower surface area (compared with smaller spheroids and ultimately single cells) in addition to the lag time for the compound to reach the biotransformation site. Another factor that might affect the clearance rate is the bioavailability of the compound that might be dependent on the amount of protein present in the 50- and 100-spheroid sample solution. To address this, the present study tested the retention capacity of pyrene in L-15 by using different BSA concentrations. It was found that protein content of 1% BSA had a slightly higher capacity of keeping the amount of spiked-in pyrene stable over time in the L-15 media compared with 0.1% BSA (Supplemental Data, Figure S1). Nevertheless, further research would be required to reach a definitive conclusion as to why this difference in clearance rate is occurring. Until then, it cannot be concluded that the chosen number of spheroids (100 spheroids per reaction) yielded the optimal depletion rate of pyrene during the 30 h of testing. Consequently, to make this bioassay feasible and possibly applicable as a future compound biotransformation method, the lowest number of spheroids yielding the most reproducible data was used.

To obtain high biotransformation efficiency, only mature spheroids (>8 d post-isolation) were used in the present study (ages 10–18 d post-isolation) because they have been shown to have an increased activity of proteins associated with metabolite excretion through the cellular efflux transporters (e.g., proteins of the adenosine triphosphate-binding cassette; Xu et al. 2005; Uchea et al. 2015), compared with immature (5–7 d post-isolation) hepatic spheroid cultures of trout (Uchea et al. 2015). The selected 3D spheroids demonstrated high metabolic activity with measurable depletion of pyrene after only 2 h of exposure, displaying a log-linear depletion up to 30 h of exposure. Biotransformation of pyrene had previously been expected based on the continuous compound clearance in in vitro substrate depletion assays such as primary hepatocyte and S9 fractions (Nichols et al. 2018); however, analytical verification of, for example, formation of metabolites has been warranted. In the present study, we confirmed analytically that pyrene was taken up and biotransformed into the metabolite OH-PYR-Glu by the hepatic spheroids. The 3D spheroids exhibited a continuous formation of OH-PYR-Glu until 30 h of exposure to pyrene. The quantification of OH-PYR-Glu was, nevertheless, quite uncertain because of the short retention time used in the present analytical method, although the time-dependent increase identified the metabolic activity of the spheroids. Surprisingly, there was no detection of the phase I metabolite OH-PYR in any of the samples. To address this, a deconjugation procedure of β-glucuronidase/aryl sulfatase was applied to identify the possible metabolites formed during the pyrene exposure. This deconjugation procedure identified and verified that there was a formation of OH-PYR increasing over the full duration of exposure. However, the lack of identification in nondeconjugated samples suggests that the subcellular conjugation process converting OH-PYR into OH-PYR-Glu is rapid enough that levels of OH-PYR are below the limit of analytical quantification (Saengtienchai et al. 2015). This is

further supported by the fact that the majority of the metabolites found in the hepatic spheroid samples were OH-PYR-Glu, which together with pyrene sulphate are the 2 major conjugation metabolites expected in in vivo fish liver (Ikenaka et al. 2013). Pyrene sulphate was not specifically analyzed in the present study but the chemical analysis highlighted an unidentified pyrene metabolite peak on the chromatogram. This peak was possibly OH-PYR sulphate because the retention time was longer (4.8 min) compared with the glucuronide (4.2 min), which corresponds well with previous literature in both fish and rats (Ikenaka et al. 2013; Saengtienchai et al. 2015). Our results revealed the 3D spheroids' ability to biotransform pyrene into both phase I OH-PYR and phase II glucuronide and possibly sulphate metabolites, as previously described for in vivo pyrene-exposed fish (Ikenaka et al. 2013). However, because we did not specifically investigate pyrene sulphate, this conclusion remains to be confirmed.

Calculation of in vitro intrinsic clearance ($CL_{in\ vitro}$) for the 3D spheroids reported very similar values to the recently published data for cryopreserved hepatocytes (Nichols et al. 2018; Organisation for Economic Co-operation and Development 2018). Established in vitro intrinsic CL assays using S9 fractions and primary hepatocytes (fresh and cryopreserved) have displayed reproducible elimination rates within 14 and 50 min, when incubated with 25 nM pyrene. The hepatic 3D spheroids require a longer duration of exposure (30 h) to biotransform pyrene into its metabolites OH-PYR and OH-PYR-Glu, as shown both by the present study and an earlier study (Baron et al. 2017). Similar to spheroids, single cells (e.g., hepatocytes) have been recommended to require a prolonged duration of exposure compared with S9 fractions because of co-factor limitations and/or rate-limiting cell permeability (Fay et al. 2017). The larger size (Ø 90–150 μm) and lower total surface area of the spheroids compared with single hepatocytes (Ø 16.7 ± 0.4 μm; Moutou et al. 1997) may also be a reason for lower clearance rate of pyrene in spheroids, although this is still to be experimentally verified. Despite this, the advantage of using spheroid cultures compared with subcellular (S9 fraction) assays is that the former better represent the in vivo system because the compound needs to be transported across cell membranes (Uchea et al. 2015). This feature is lacking in currently used S9 fraction substrate depletion assays, where elimination is expected (Johanning et al. 2012). Biotransformation of slowly metabolized compounds (e.g., methoxychlor) has proven challenging for both the S9 fractions and the primary hepatocyte bioassay because depletion rates are close to the lower limit of measurable chemical quantification (Nichols et al. 2018). This is yet another advantage of the hepatic rainbow trout spheroids because the bioassay is viable for a prolonged exposure duration (≥72 h; Baron et al. 2017), thus making them applicable for testing of more challenging (e.g., highly hydrophobic, persistent) compounds. However, the lowest limit of $CL_{in\ vitro}$ rate is still to be experimentally established for all the in vitro depletion bioassays (primary hepatocytes, S9 fractions, and the 3D spheroids).

The metabolic competence of spheroids used in the present study is comparable with previous in vitro studies using cryopreserved hepatocytes (Table 1). There was however a difference in biotransformation of pyrene between the present study and previous studies for both fresh and cryopreserved primary hepatocytes incubated with 25 and 250 nM pyrene (Fay et al. 2017; Nichols et al. 2018). The recently published ring trial study reported that cryopreserved hepatocytes yielded a factor of 1.8 times higher $CL_{in\ vitro}$ than the present study (Nichols et al. 2018). The same study estimated $CL_{in\ vivo}$ for S9 fractions (2603 mL/h/g liver) to be 2.6 times higher than the hepatocyte-based assays. This suggests that the S9 fraction is more efficient than the cryopreserved hepatocyte (Nichols et al. 2018) and the spheroid-based assays presented herein.

The interbatch variability was fairly high in the present study (coefficient of variation 18–58%) but comparable with other studies reporting intercell batch variations of 30 to 50% when using cryopreserved primary hepatocytes in metabolic clearance rate assays (Mingoia et al. 2010). Nevertheless, when compared with recent pyrene depletion studies using cryopreserved hepatocytes (coefficient of variation 27.9 ± 11.0%; Nichols et al. 2018) the present study had a higher coefficient of variation percentage. Some of the variability may be attributed to the different cell batches used and minor differences in the number of spheroids per replicate, in addition to uncertainties in the analytical quantification of low concentrations of pyrene. One explanation for the low intralaboratory and interlaboratory variability reported by Nichols et al. (2018) may be that the study was using a more homogenous sample of hepatocytes as each mixed batch consisted of 7 animals of different gender, yielding a possibly more representative response than when testing individual cell batches. In addition, previously described in vitro depletion assays (cryopreserved and S9 fraction) consisted of technical replicates that were subsampled from one sample over time to establish the compounds' specific elimination rate (Fay et al. 2017; Nichols et al. 2018; Organisation for Economic Co-operation and Development 2018). The present study did not perform subsamples but instead sampled up to 4 technical replicates per time point, which probably contributed to most of the variability observed.

Other features that might give rise to differences among experimental studies using chemical depletion bioassays might result from the sampling method. Herein, the application of the 2 different sampling procedures displayed similar elimination rates during the test (Figures 2 and 3). However, SP1 was not able to distinguish between adsorbed and dissolved pyrene (free, bound-to-media constituents, and within spheroid) in the test system (Figure 2). Despite the substantial amount of pyrene adhering to the glass vial and thus being less available for the spheroids, this was not the rate-limiting factor for metabolism of pyrene (Figure 3 and Supplemental Data, Figure S4). Other studies using cryopreserved primary hepatocytes (Nichols et al. 2018) have not reported issues with recovery of dissolved pyrene during their exposures. This might be caused by the presence of higher dissolved protein content (hepatocytes 2.85 ± 0.34 mg/mL; Nichols et al. 2018) in the exposure vial than in the present study (spheroids 0.0211 mg/mL; calculations based on Baron et al. 2012). This was further investigated in the present study by measuring total amount of pyrene in the media in the presence of a protein content similar to that reported for hepatocytes by Nichols et al. (2018; BSA 0.1%, 2.65 mg/mL). The data showed that homogenously

dissolved BSA 0.1% had a 1.4 to 1.7 times higher retention of the pyrene in solution than in L-15 alone during 6 h of exposure. These results display the potential challenges of using 3D spheroids when testing highly hydrophobic compounds because substantial amounts may be less available for the spheroids (as a result of fewer and densely accumulated cells) during the whole duration of the test. Pyrene is a small molecule with only an intermediate hydrophobicity, and thus does not pose the same challenges as larger and more hydrophobic compounds. An example of such a compound would be methoxychlor, which has been shown to have limited membrane permeability that influences biotransformation inside cells (Dimitrov et al. 2003; Johanning et al. 2012).

In summary, the present study illustrated the importance of verifying the test compound's bioavailability during the whole test to account for how much of the test compound is available to the spheroids. Many studies based on the metabolic clearance assume that all spiked chemical is bioavailable for the cells during the full duration of the test (Mingoia et al. 2010; Fay et al. 2014a, 2014b; Fay et al. 2017; Nichols et al. 2018). Although this is not an issue for pyrene, slowly metabolized substances that might have proven difficult to assess with S9 fractions and freshly prepared hepatocytes requiring longer exposure durations before biotransformation might be better assessed using 3D spheroids because they can be exposed for a longer period of time (>72 h) and are viable for >30 d. Whereas recognizing that further development of this assay requires additional compounds to be assayed and interlaboratory ring trials to be performed, at this time 3D spheroids could be considered complementary to the other in vitro depletion assays. Ultimately, its use in a weight-of-evidence approach such as the tiered assessment strategy to improve bioaccumulation assessments of chemicals recommended by Lillicrap et al. (2016b) is warranted.

CONCLUSIONS

The present study determined that 3D hepatic spheroids from rainbow trout are highly metabolically active because they biotransformed pyrene during 30 h of exposure at an intrinsic CL rate comparable with other in vitro depletion assays. In addition, the 3D spheroids displayed efficient biotransformation of pyrene into one of its metabolites (OH-PYR-Glu) during the full duration of exposure. Compared with other in vitro depletion assays, a major benefit of using 3D spheroids is that their microenvironment is more similar to the in vivo tissue. Moreover, 3D spheroids permit considerably longer exposure durations. The present study suggested that the 3D spheroid model might contribute valuable data that also might improve the prediction of a compound's bioconcentration potential in vitro, and further extrapolation into in vivo.

Supplemental Data—The Supplemental Data are available on the Wiley Online Library at DOI: 10.1002/etc.4476.

Acknowledgment—The authors are grateful to L. Fredriksen for her contribution in establishing the 3D spheroid bioassay at the Norwegian Institute for Water Research. We thank J. Nichols for his input into chemical analysis and discussion, and we are indebted to S. Brooks for critically reviewing the present study before submission. The authors would also like to acknowledge the Norwegian Research Council (NRC Project No. 160016) for funding to conduct the work presented herein.

Disclaimer—The views, conclusions, and recommendations expressed in the present study are those of the authors and do not necessarily represent the views or policies of the Norwegian Institute for Water Research.

Data Accessibility—Data obtained during the present study are accessible from the corresponding author (mhu@niva.no).

REFERENCES

Arnot JA, Gobas FA. 2006. A review of bioconcentration factor (BCF) and bioaccumulation factor (BAF) assessments for organic chemicals in aquatic organisms. *Environ Rev* 14:257–297.

Arnot JA, Meylan W, Tunkel J, Howard PH, Mackay D, Bonnell M, Boethling RS. 2009. A quantitative structure–activity relationship for predicting metabolic biotransformation rates for organic chemicals in fish. *Environ Toxicol Chem* 28:1168–1177.

Baron MG, Mintram KS, Owen SF, Hetheridge MJ, Moody AJ, Purcell WM, Jackson SK, Jha AN. 2017. Pharmaceutical metabolism in fish: Using a 3-D hepatic in vitro model to assess clearance. *PLoS One* 12:e0168837.

Baron MG, Purcell WM, Jackson SK, Owen SF, Jha AN. 2012. Towards a more representative in vitro method for fish ecotoxicology: Morphological and biochemical characterisation of three-dimensional spheroidal hepatocytes. *Ecotoxicology* 21:2419–2429.

Dimitrov SD, Dimitrova NC, Walker JD, Veith GD, Mekenyan OG. 2003. Bioconcentration potential predictions based on molecular attributes—An early warning approach for chemicals found in humans, birds, fish and wildlife. *QSAR Comb Sci* 22:58–68.

Elliott NT, Yuan F. 2011. A review of three-dimensional in vitro tissue models for drug discovery and transport studies. *J Pharm Sci* 100:59–74.

Embry M, Bernhard M, Davis J, Domoradzki J, Fay K, Bischof I, Halder M, Han X, Hu J, Johanning K, Laue H, Nabb D, Nichols JW, Schlechtriem C, Segner H, Tollefsen K, Van der Wal L, Weeks JA. 2015. In vitro fish hepatic metabolism: Overview of ring-trial to evaluate transferability, intra- and inter-laboratory reproducibility. SETAC Europe 25th Annual Meeting, Barcelona, Spain, May 3–7, 2015.

Fay KA, Fitzsimmons PN, Hoffman AD, Nichols JW. 2014a. Optimizing the use of rainbow trout hepatocytes for bioaccumulation assessments with fish. *Xenobiotica* 44:345–351.

Fay KA, Mingoia RT, Goeritz I, Nabb DL, Hoffman AD, Ferrell BD, Peterson HM, Nichols JW, Segner H, Han X. 2014b. Intra- and interlaboratory reliability of a cryopreserved trout hepatocyte assay for the prediction of chemical bioaccumulation potential. *Environ Sci Technol* 48:8170–8178.

Fay KA, Fitzsimmons PN, Hoffman AD, Nichols JW. 2017. Comparison of trout hepatocytes and liver S9 fractions as in vitro models for predicting hepatic clearance in fish. *Environ Toxicol Chem* 36:463–471.

Hoffmann OI, Ilmberger C, Magosch S, Joka M, Jauch KW, Mayer B. 2015. Impact of the spheroid model complexity on drug response. *J Biotechnol* 205:14–23.

Ikenaka Y, Oguri M, Saengtienchai A, Nakayama SM, Ijiri S, Ishizuka M. 2013. Characterization of phase-II conjugation reaction of polycyclic aromatic hydrocarbons in fish species: Unique pyrene metabolism and species specificity observed in fish species. *Environ Toxicol Pharmacol* 36:567–578.

Johanning K, Hancock G, Escher B, Adekola A, Bernhard M, Cowan-Ellsberry C, Domoradzki J, Dyer S, Eickhoff C, Ernhardt S, Fitzsimmons P, Halder M, Nichols J, Rutishauser S, Sharpe A, Segner H, Schultz I, Embry M. 2012. In vitro metabolism using rainbow trout liver S9. Summary report of the HESI Bioaccumulation Committee. Washington, DC, USA.

Kammann U, Askem C, Dabrowska H, Grung M, Kirby MF, Koivisto P, Lucas C, McKenzie M, Meier S, Robinson C. 2013. Interlaboratory proficiency testing for measurement of the polycyclic aromatic hydrocarbon

metabolite 1-hydroxypyrene in fish bile for marine environmental monitoring. *J AOAC Int* 96:635–641.

Kyffin JA, Sharma P, Leedale J, Colley HE, Murdoch C, Harding AL, Mistry P, Webb SD. 2019. Characterisation of a functional rat hepatocyte spheroid model. *Toxicol In Vitro* 55:160–172.

Kyffin JA, Sharma P, Leedale J, Colley HE, Murdoch C, Mistry P, Webb SD. 2018. Impact of cell types and culture methods on the functionality of in vitro liver systems—A review of cell systems for hepatotoxicity assessment. *Toxicol In Vitro* 48:262–275.

Lammel T, Tsoukatou G, Jellinek J, Sturve J. 2019. Development of three-dimensional (3D) spheroid cultures of the continuous rainbow trout liver cell line RTL-W1. *Ecotox Environ Safe* 167:250–258.

Langan LM, Owen SF, Trznadel M, Dodd NJF, Jackson SK, Purcell WM, Jha AN. 2018. Spheroid size does not impact metabolism of the β-blocker propranolol in 3D intestinal fish model. *Front Pharmacol* 9:947.

Lillicrap A, Belanger S, Burden N, Pasquier DD, Embry MR, Halder M, Lampi MA, Lee L, Norberg-King T, Rattner BA. 2016a. Alternative approaches to vertebrate ecotoxicity tests in the 21st century: A review of developments over the last 2 decades and current status. *Environ Toxicol Chem* 35:2637–2646.

Lillicrap A, Springer T, Tyler CR. 2016b. A tiered assessment strategy for more effective evaluation of bioaccumulation of chemicals in fish. *Regul Toxicol Pharmacol* 75:20–26.

Lowry OH, Rosebrough NJ, Farr AL, Randall RJ. 1951. Protein measurement with the Folin phenol reagent. *J Biol Chem* 193:265–275.

Mingoia RT, Glover KP, Nabb DL, Yang C-H, Snajdr SI, Han X. 2010. Cryopreserved hepatocytes from rainbow trout (Oncorhynchus mykiss): A validation study to support their application in bioaccumulation assessment. *Environ Sci Technol* 44:3052–3058.

Moutou K, Braunbeck T, Houlihan D. 1997. Quantitative analysis of alterations in liver ultrastructure of rainbow trout Oncorhynchus mykiss after administration of the aquaculture antibacterials oxolinic acid and flumequine. *Dis Aquat Organ* 29:21–34.

Nichols J, Fay K, Bernhard MJ, Bischof I, Davis J, Halder M, Hu J, Johanning K, Laue H, Nabb D. 2018. Reliability of in vitro methods used to measure intrinsic clearance of hydrophobic organic chemicals by rainbow trout: Results of an international ring trial. *Toxicol Sci* 164:563–575.

Organisation for Economic Co-operation and Development. 2018. Test Nos. 319A, 319B: Multi-laboratory ring trial to support development of OECD test guidelines on determination of in vitro intrinsic clearance using cryopreserved rainbow trout hepatocytes and liver S9 sub-cellular fractions. *OECD Guidelines for the Testing of Chemicals*. Paris, France.

Papa E, Van der Wal L, Arnot JA, Gramatica P. 2014. Metabolic biotransformation half-lives in fish: QSAR modeling and consensus analysis. *Sci Total Environ* 470-471:1040–1046.

Qian Y, Posch T, Schmidt TC. 2011. Sorption of polycyclic aromatic hydrocarbons (PAHs) on glass surfaces. *Chemosphere* 82:859–865.

Ramaiahgari SC, Waidyanatha S, Dixon D, DeVito MJ, Paules RS, Ferguson SS. 2017. From the Cover: Three-dimensional (3D) HepaRG spheroid model with physiologically relevant xenobiotic metabolism competence and hepatocyte functionality for liver toxicity screening. *Toxicol Sci* 159:124–136.

Remington JP. 2006. *Remington: The Science and Practice of Pharmacy*, 21st ed, Vols 1 and 2. Lippincott Williams & Wilkins, Philadelphia, PA, USA.

Rovida C, Hartung T. 2009. Re-evaluation of animal numbers and costs for in vivo tests to accomplish REACH legislation requirements for chemicals—A report by the Transatlantic Think Tank for Toxicology (t^4). *ALTEX* 26:187–208.

Saengtienchai A, Ikenaka Y, Darwish WS, Nakayama SMM, Mizukawa H, Ishizuka M. 2015. Characterization and tissue distribution of conjugated metabolites of pyrene in the rat. *J Vet Med Sci* 77:1261–1267.

Schirmer K. 2006. Proposal to improve vertebrate cell cultures to establish them as substitutes for the regulatory testing of chemicals and effluents using fish. *Toxicology* 224:163–183.

Scholz S, Sela E, Blaha L, Braunbeck T, Galay-Burgos M, García-Franco M, Guinea J, Klüver N, Schirmer K, Tanneberger K, Tobor-Kapłon M, Witters H, Belanger S, Benfrenati E, Creton S, Cronin MTD, Eggen RIL, Embry M, Ekman D, Gourmelon A, Halder M, Hardy B, Hartung T, Hubesch B, Jungmann D, Lampi MA, Lee L, Léonard M, Küster E, Lillicrap A, Luckenbach T, Mark AJ, Navas JM, Peijnenburg W, Repetto G, Salinas E, Schüürmann G, Spielmann H, Tollefsen KE, Walter-Rohde S, Whale G, Wheeler JR, Winter MJ. 2013. A European perspective on alternatives to animal testing for environmental hazard identification and risk assessment. *Regul Toxicol Pharmacol* 67:506–530.

Stadnicka-Michalak J, Weiss FT, Fischer M, Tanneberger K, Schirmer K. 2018. Biotransformation of benzo [a] pyrene by three rainbow trout (Onchorhynchus mykiss) cell lines and extrapolation to derive a fish bioconcentration factor. *Environ Sci Technol* 52:3091–3100.

Tollefsen K-E, Mathisen R, Stenersen J. 2003. Induction of vitellogenin synthesis in an Atlantic salmon (Salmo salar) hepatocyte culture: A sensitive in vitro bioassay for the oestrogenic and anti-oestrogenic activity of chemicals. *Biomarkers* 8:394–407.

Uchea C, Owen SF, Chipman JK. 2015. Functional xenobiotic metabolism and efflux transporters in trout hepatocyte spheroid cultures. *Toxicol Res* 4:494–507.

Van der Oost R, Beyer J, Vermeulen NPE. 2003. Fish bioaccumulation and biomarkers in environmental risk assessment: A review. *Environ Toxicol Pharmacol* 13:57–149.

Xu C, Li CY-T, Kong A-NT. 2005. Induction of phase I, II and III drug metabolism/transport by xenobiotics. *Arch Pharm Res* 28:249–268.

